

# The Cepheid impostor HD 18391 and its anonymous parent cluster

D.G. Turner<sup>1,3\*</sup>, V.V. Kovtyukh<sup>2</sup>, D.J. Majaess<sup>1</sup>, D.J. Lane<sup>1</sup>, and K.E. Moncrieff<sup>1</sup>

<sup>1</sup> Department of Astronomy and Physics, Saint Mary's University, Halifax, Nova Scotia B3H 3C3, Canada

<sup>2</sup> Astronomical Observatory, Odessa National University, T. G. Shevchenko Park, 65014, Odessa, Ukraine

<sup>3</sup> Visiting Astronomer, Dominion Astrophysical Observatory, Herzberg Institute of Astrophysics, National Research Council of Canada

Received 2009 Mar 26, accepted 2009 Jul 6

Published online 2009 Sep 20

**Key words** Cepheids – open clusters and associations: individual – techniques: photometric

New and existing photometry for the G0 Ia supergiant HD 18391 is analyzed in order to confirm the nature of the variability previously detected in the star, which lies off the hot edge of the Cepheid instability strip. Small-amplitude variability at a level of  $\Delta V = 0.016 \pm 0.002$  is indicated, with a period of  $P = 123^d.04 \pm 0^d.06$ . A weaker second signal may be present at  $P = 177^d.84 \pm 0^d.18$  with  $\Delta V = 0.007 \pm 0.002$ , likely corresponding to fundamental mode pulsation if the primary signal represents overtone pulsation ( $123.04/177.84 = 0.69$ ). The star, with a spectroscopic reddening of  $E_{B-V} = 1.02 \pm 0.003$ , is associated with heavily-reddened B-type stars in its immediate vicinity that appear to be outlying members of an anonymous young cluster centered  $\sim 10'$  to the west and  $1661 \pm 73$  pc distant. The cluster has nuclear and coronal radii of  $r_n = 3.5'$  and  $R_c = 14'$ , respectively, while the parameters for HD 18391 derived from membership in the cluster with its outlying B stars are consistent with those implied by its Cepheid-like pulsation, provided that it follows the semi-period-luminosity relation expected of such objects. Its inferred luminosity as a cluster member is  $M_V = -7.76 \pm 0.10$ , its age  $(9 \pm 1) \times 10^6$  years, and its evolutionary mass  $\sim 19 M_\odot$ . HD 18391 is not a classical Cepheid, yet it follows the Cepheid period-luminosity relation closely, much like another Cepheid impostor, V810 Cen.

© 2009 WILEY-VCH Verlag GmbH & Co. KGaA, Weinheim

## 1 Introduction

The Cepheid instability strip is well recognized as the principal region of the H-R diagram occupied by luminous variable stars of spectral types F, G, and K. Less well known is the region blueward and at higher luminosity than the Cepheid instability strip occupied by a variety of stars, typically of luminosity classes Ia to Ib, exhibiting variability and microvariability at much smaller amplitudes (Maeder & Rufener 1972; Rufener et al. 1978; Rufener & Bartholdi 1982). Such stars appear to obey relationships, as a function of spectral type or color, between their luminosities and semi-periods of variability (Burki 1978b; Burki et al. 1978) that, with the inclusion of amplitude as an additional parameter, are adequately explained by evolutionary models of massive stars that incorporate mass loss (Maeder 1980).

The G0 Ia supergiant HD 18391 (Nassau & Morgan 1952) has been used previously to characterize the cool end of the above relationships, tied to observations by Rufener et al. (1978). It is listed as a potential member of the double cluster h & χ Persei (Schmidt 1984), as well as Cas OB6 (Stothers 1972). The star's broad spectral lines were remarked upon by Redman (1930) and Griffin (1970), although that feature appears to be related to high luminosity in late-type stars (Imhoff 1977). Broad band *UBV* photoelectric photometry for the star was tabulated by Argue

(1966), based upon 4 observations from Kitt Peak National Observatory. Additional *UBV* photometry is given by Haug (1970), but the evidence for variability lies in the observations of Rufener et al. (1978), in which the star was observed to increase gradually in brightness over an interval of 85 nights during the winter of 1972–1973.

Unlike other stars defining the semi-period-luminosity-color relation for supergiants (Burki 1978b), the semi-period of  $\geq 84$  days for HD 18391 was estimated from a single incomplete cycle, and is not well established. Our interest in HD 18391 arose from its spectroscopic parameters, which enabled its interstellar reddening to be estimated using a newly-developed technique (Kovtyukh 2007; Kovtyukh et al. 2008). The star's location in the spectroscopic H-R diagram (Fig. 1) suggests a possible link to the Cepheid instability strip, which raises an intriguing question. Does the instability strip for Galactic Cepheids extend to pulsating GK supergiants like those in the Magellanic Clouds, where pulsation periods on the order of 100 days are not unusual? The present investigation was initiated in order to examine that question in greater detail.

\* Corresponding author: turner@ap.smu.ca

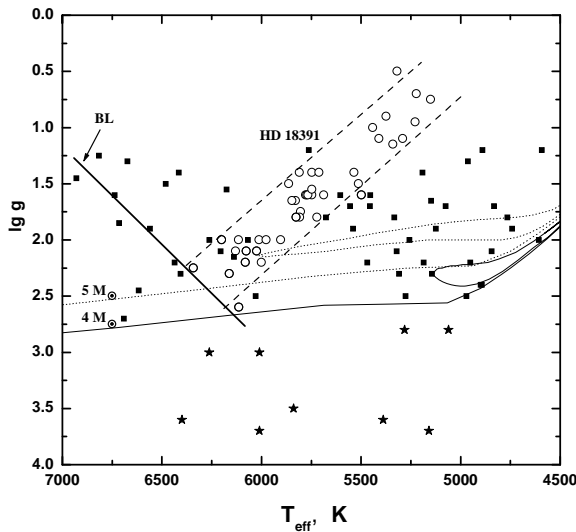


**Fig. 1** The location of HD 18391 (numbered filled square) relative to other FGK giants and supergiants (other filled squares), known Cepheid variables (open circles), and the instability strip (dashed lines) in a HR diagram that plots surface gravity versus effective temperature. Evolutionary tracks are depicted for stars of 4 and  $5 M_{\odot}$ , and “BL” denotes the edge of the blue loop evolutionary stage.

## 2 Observations and air mass corrections

The present study is based upon photometric observations of the brightness of HD 18391, as well as a detailed stellar atmosphere study of the star by Kovtyukh (2007) and Kovtyukh et al. (2008) that generated the spectroscopic parameter  $T_{\text{eff}} = 5775$  K using line ratio techniques, as well as  $\log g = 1.2$ , metallicity  $[\text{Fe}/\text{H}] = 0.02$ , and microturbulent velocity  $12.0 \text{ km s}^{-1}$ . New CCD  $V$ -band differential photometry for HD 18391 was obtained on 101 nights between July 2007 and April 2009 using the 28-cm Schmidt-Cassegrain telescope of the semi-automated Abbey Ridge Observatory (ARO) located in Stillwater Lake, just outside of Halifax, Nova Scotia (see Majaess et al. 2008). All-sky CCD  $BV$  photometry for the same field was also obtained on the photometric nights of 2007 October 22, 23, and 26, using stars in the nearby open cluster NGC 225 as reference standards (Hoag et al. 1961). Finally, we obtained CCD spectra in October 2008 for some luminous stars in the immediate vicinity of HD 18391, using the Cassegrain spectrograph on the Plaskett telescope of the Dominion Astrophysical Observatory, at a dispersion of  $60 \text{ \AA mm}^{-1}$ .

Differential photometry for HD 18391 was obtained relative to HD 18327 (A0), with BD+57°668 (G0: V) serving as a check star. All-sky photometry for the three stars yielded the results summarized in Table 1, where comparison estimates for the magnitudes and colors are taken from mean Tycho  $V$ -band observations (Perryman et al. 1997), Argue (1966), and Haug (1970). The mean Tycho  $V$  magni-

**Table 1**  $BV$  magnitudes and colors for program objects.

Star	$V$	$B - V$	Source
HD 18391 (G0 Ia)	$6.937 \pm 0.004$	$1.966 \pm 0.003$	This paper
	$6.936 \pm 0.005$	$1.982 \pm 0.015$	Tycho <sup>1</sup>
	$6.890 \pm \dots$	$1.950 \pm \dots$	Argue 1966
	$6.890 \pm \dots$	$1.930 \pm \dots$	Haug 1970
HD 18327 (A0)	$8.729 \pm 0.010$	$0.222 \pm 0.013$	This paper
	$8.732 \pm 0.011$	$0.211 \pm 0.015$	Tycho <sup>1</sup>
BD+57°668 (G0 V:)	$9.797 \pm 0.001$	$0.605 \pm 0.007$	This paper
	$9.827 \pm 0.019$	$0.676 \pm 0.031$	Tycho <sup>1</sup>

<sup>1</sup>Perryman et al. 1997

tude for HD 18391 was adjusted according to the precepts of Bessell (2000), but only half of the suggested correction to  $B - V$  color was used, otherwise the result would be significantly bluer than the values found by Argue (1966), Haug (1970), and this study. The mean Tycho values for HD 18327 and BD+57°668, which are much bluer, are cited without adjustment.

Because the comparison stars are much bluer than HD 18391, it was necessary to adjust the differential photometry for air mass effects, atmospheric extinction being well known to diminish the brightness of blue stars by larger amounts than that of red stars as air mass increases. HD 18391 is a yellow star of very large reddening (Kovtyukh et al. 2008), so its brightness relative to bluer comparison stars would appear to increase artificially when viewed through large air masses if such corrections were not made. Given the low level of light variability in HD 18391, tests for such an effect are essential to confirm that any detected variability originates in the star rather than Earth’s atmosphere.

Such an effect can be seen in differential photometry by Fuentes et al. (2006) from Mt. Hopkins for the high latitude hypervelocity blue star SDSS J090744.99+024506.8 (HVS) at  $9^{\text{h}}07^{\text{m}}45^{\text{s}}.0$ ,  $+2^{\circ}45'07''$  (J2000). Fuentes et al. (2006) concluded that the star was a small amplitude variable because their differential CCD photometry relative to redder field stars in its vicinity indicated a brightness decrease on two nights of observation, coincident with an increase in the star’s air mass. Temporal plots of the brightness of HVS on the two nights are replotted in Fig. 2 to display its changing brightness as a function of air mass  $X$ . For comparison stars with colors typical of G dwarfs relative to HVS, our experience with photometry from Kitt Peak suggests that the expected trends should have functional dependences of about  $-0.03$  for  $g$ -band observations and  $-0.01$  for  $r$ -band observations. The observed dependences are  $-0.027$  and  $-0.009$ , respectively. The decreasing brightness of HVS as a function of increasing air mass is therefore exactly what is predicted for a blue star being compared with redder comparison stars, implying that its light variations are not intrinsic to the star.

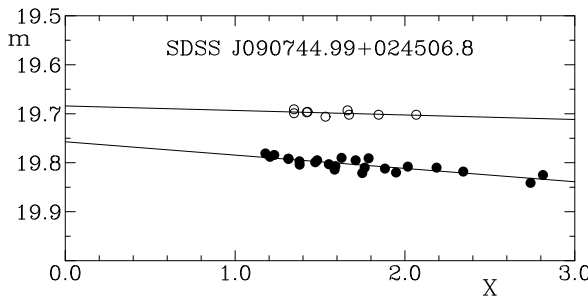


**Fig. 2** The dependence of observations by Fuentes et al. (2006) for SDSS J090744.99+024506.8 on air mass  $X$ . Filled symbols represent  $g$ -band observations, open symbols  $r$ -band observations offset by  $-0.1$ . Straight lines are best fits to the observed trends, with residual scatter of  $\pm 0.008$  in  $g$  and  $\pm 0.005$  in  $r$ .

The nonvariable status of HVS appears to be important to our understanding of the star, given that Fuentes et al. (2006) based their conclusion that it is a slowly-pulsating B-type main-sequence star (SPB) primarily on its purported variability. Since HVS is not variable, the original spectrum of the star obtained by Brown et al. (2005) becomes a vital diagnostic tool. The spectrum displays broad hydrogen Balmer lines that appear to terminate near H13 or H14, which normally corresponds to a surface gravity of  $\log g \simeq 4.5$  in B-type stars (e.g., Vitense 1951). That is typical of objects lying below the main sequence, such as the blue horizontal branch stars originally considered by Brown et al. (2005), and more recently by Demarque & Virani (2007), as a potential origin for the object. Perhaps that possibly should be reconsidered, given that it is vital to any conclusions regarding the dynamical origin of hypervelocity stars?

The Geneva observations for HD 18391 (Rufener et al. 1978), supplemented by a few additional unpublished observations by the group (Burki 2007), were also checked for air mass effects, despite their origin from calibrated all-sky photometry. The site of the observations is not specified in the original references, but was assumed to be Gornergrat. The  $V$ -band observations are plotted in Fig. 3 as a function of inferred air mass, where it appears that a small zero-point offset affects observations on six of the nights, most of which were designated as being of low quality. An adjustment of  $-0.025$  was adopted to bring them into agreement with the remaining observations, and the resulting data were adjusted for a small air mass term in the data (equivalent to an overly steep color dependence) and adjusted to a mean magnitude near  $V = 6.94$ , to be consistent with the present data set.

A similar plot is presented in Fig. 4 for our raw differential photometry relative to HD 18327. A zero-point offset is present midway through our data set as a result of a change in CCD detectors, which produced a change in the color dependence for the observations. There is also a small difference in air mass dependence between observations in 2007 and 2008–2009. Corrections for all such effects, an air mass

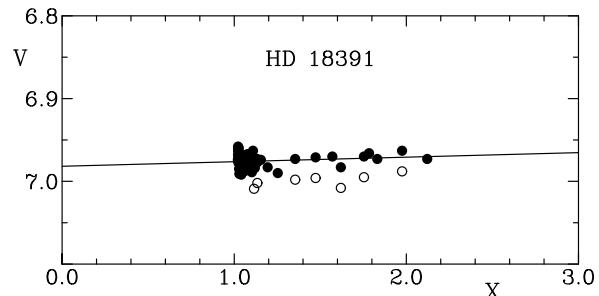


**Fig. 3** The dependence of Geneva observations for HD 18391 on air mass  $X$ . Open symbols represent data from six nights of low quality, subsequently offset by  $-0.025$  to match observations on other nights. The straight line is a best fit to the latter.

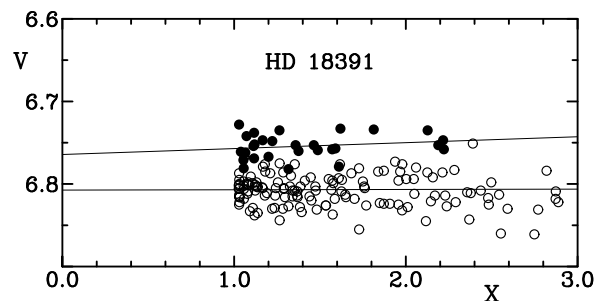


**Fig. 4** The dependence of Abbey Ridge observations for HD 18391 on air mass  $X$ . Filled symbols represent observations from the first portion of the observing period, open symbols observations made after a change in CCD detectors. Straight lines are best fits to the observed trends.

dependence, zero-point offset, and differences relative to the results of our all-sky photometry, were made to all observations, with nightly means summarized in Table 2, including a few combined observations from adjacent nights. Plots of the resulting time dependence for the Geneva, Tycho, and ARO observations are shown in Fig. 5.

### 3 Period analysis

It is not evident from the available observations that HD 18391 is a variable star. The standard deviations for the various data sets are  $\pm 0.009$  for Geneva observations,  $\pm 0.015$  for Tycho observations, and  $\pm 0.012$  for ARO data in Table 2,  $\pm 0.014$  for the individual observations. The dispersion in the ARO check star observations is  $\pm 0.016$ , which is larger than the scatter observed for HD 18391 only because the latter is 3 magnitudes brighter than the check star. Its signal therefore had a higher signal-to-noise ratio (SNR) than those for the comparison stars, and was affected less by photon statistics. Small SNRs for the comparison stars were inevitable, given that exposure times were kept short to avoid saturation of the target. The scatter for the check star also appears to be random, whereas the observations for HD 18391 display slight temporal trends. Similar observations for other stars observed at the ARO of comparable

**Table 2** *V*-band observations of HD 18391 2007–2009.

HJD	<i>V</i>	HJD	<i>V</i>	HJD	<i>V</i>
2454308.737	6.945	2454522.622	6.935	2454748.599	6.935
2454309.716	6.943	2454526.589	6.941	2454750.586	6.905
2454313.679	6.938	2454532.548	6.926	2454753.662	6.924
2454322.605	6.949	2454537.517	6.920	2454757.658	6.925
2454324.644	6.922	2454539.563	6.940	2454759.631	6.936
2454325.638	6.945	2454544.558	6.933	2454763.616	6.932
2454332.620	6.944	2454549.589	6.960	2454764.610	6.943
2454349.235	6.941	2454551.555	6.940	2454765.513	6.946
2454358.693	6.930	2454559.539	6.939	2454771.589	6.941
2454360.776	6.943	2454560.577	6.942	2454772.643	6.941
2454362.661	6.932	2454563.554	6.934	2454773.613	6.949
2454364.730	6.925	2454564.526	6.935	2454783.483	6.956
2454365.699	6.921	2454565.527	6.935	2454788.567	6.950
2454367.778	6.910	2454566.532	6.925	2454804.736	6.965
2454368.606	6.938	2454571.530	6.947	2454888.588	6.941
2454403.461	6.920	2454572.550	6.940	2454895.579	6.939
2454412.484	6.945	2454573.536	6.947	2454896.535	6.947
2454413.570	6.952	2454578.543	6.909	2454899.638	6.929
2454417.604	6.954	2454701.568	6.939	2454901.607	6.941
2454429.452	6.966	2454702.543	6.948	2454903.570	6.959
2454433.478	6.951	2454714.763	6.929	2454904.574	6.958
2454453.496	6.945	2454718.651	6.937	2454905.636	6.940
2454456.451	6.935	2454725.732	6.932	2454906.534	6.932
2454457.451	6.937	2454727.559	6.945	2454907.575	6.944
2454489.487	6.934	2454728.744	6.898	2454908.677	6.939
2454492.680	6.953	2454729.653	6.929	2454912.574	6.958
2454497.745	6.940	2454730.608	6.932	2454931.573	6.949
2454499.496	6.937	2454731.667	6.915	2454936.592	6.953
2454501.545	6.944	2454732.662	6.938	2454937.577	6.955
2454516.495	6.942	2454734.652	6.928	2454941.564	6.952
2454517.496	6.944	2454742.777	6.933	2454946.572	6.943
2454518.498	6.945	2454746.627	6.906		
2454521.501	6.945	2454747.629	6.909		

brightness to HD 18391 exhibit smaller dispersion, typically about  $\pm 0.008$ , but the main conclusion is that any variability in HD 18391 is at best marginally detectable in existing observations. Previous conclusions by Rufener et al. (1978) regarding the variability of HD 18391 may therefore have been affected by the small air mass effect noted earlier.

Despite uncertainties about the quality of the different data sets, the observations were analyzed using various routines available in the PERANSO software package of Vanmunster (2006), which includes the CLEANest routine (Foster 1995). Fifteen different period finding routines were used with the combined observations, with the average value for the most significant period from twelve of them being  $P = 123^d.04 \pm 0^d.06$  s.d. A similar analysis of observations for the ARO check star, BD+57°668, was made as a consistency check, yielding a dominant period at  $P \approx 102$  days but without producing a realistic light curve.

The resulting light curve for HD 18391 fits an ephemeris given by

$$\text{HJD}_{\text{max}} = 2441695.497 + 123.04 E, \quad (1)$$

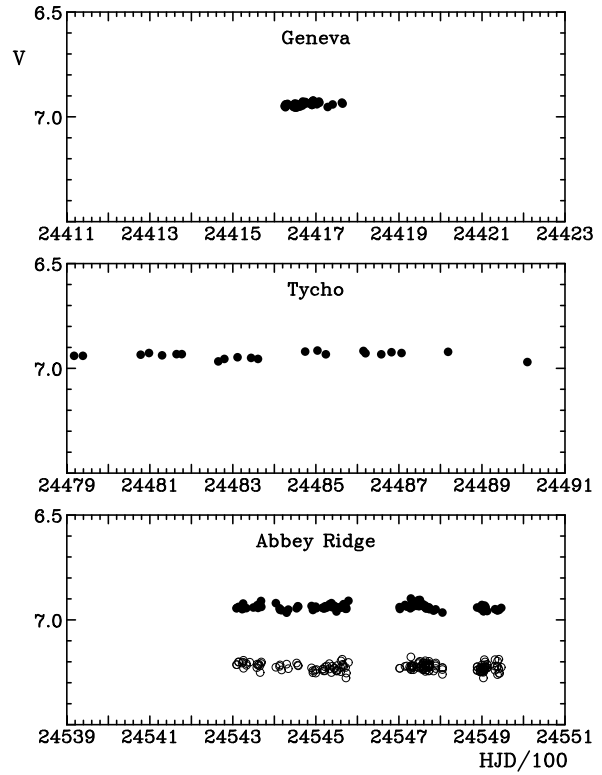


**Fig. 5** Combined observations for HD 18391 from Rufener et al. (1978) and Burki (2007), *top*, Perryman et al. (1997), *middle*, and this paper (*bottom*) plotted temporally. Open symbols in the bottom plot represent observations of the check star for the Abbey Ridge observations, offset by  $-2.35$ .

where  $E$  is the number of elapsed cycles. It is displayed in Fig. 6. The inferred light amplitude is small,  $\Delta V = 0.016 \pm 0.002$ , comparable to the scatter in the observations and marginally significant, and perhaps unusual given that pulsation amplitude typically increases with rate of mass loss and luminosity in variable supergiants (Maeder 1980). The lack of significant light variability for HD 18391 presumably implies a small rate of mass loss or strong pulsational damping by convection.

A second signal appears in the data at  $P = 177^d.84 \pm 0^d.18$  s.d. after removal of the primary signal. The signal is weak, but may be real, given that it corresponds with expectations for fundamental mode pulsation if the 123 d signal originates from overtone pulsation ( $123.04/177.84 = 0.69$ ). The ephemeris for the second signal is

$$\text{HJD}_{\text{max}} = 2441735.442 + 177.84 E, \quad (2)$$

with a light amplitude of  $\Delta V = 0.007 \pm 0.002$ . The light curve for the prewhitened observations with that period is shown in the lower portion of Fig. 6.

Conceivably some of the residual scatter in the light curves of Fig. 6 results from additional periodicities in the observations, temporal changes in light amplitude, or to rapid period changes in the star's pulsation. HD 18391 displays abundance patterns typical of stars evolving towards a first crossing of the Cepheid instability strip, including a

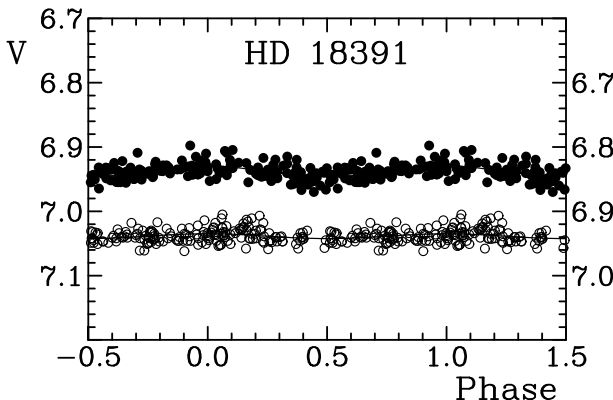


**Fig. 6** The resulting light curve for HD 18391 (filled circles) from the adopted ephemeris for  $P = 123^{\text{d}}.04$  (upper), along with the best-fitting sine wave. Open circles represent the prewhitened observations phased to  $P = 177^{\text{d}}.84$  relative to the right-hand scale.

strong lithium feature (Kovtyukh et al. 2005). As such, radial pulsation in the star should undergo period increases of several hours per year (e.g., Turner et al. 2006a), complicating the analysis significantly. The presence of a second period is remarkably similar to what is observed in V810 Cen, a F8 Ia supergiant similar in nature to HD 18391 pulsating with periods of 153 and 104 days and displaying temporal changes in light amplitude (Keinzel et al. 1998; Burki 2006). The light amplitude of HD 18391 is an order of magnitude smaller than that of V810 Cen, so additional observations and long-term monitoring are crucial to search for similar effects, as well as to confirm the small-amplitude variability implied by observations to date.

#### 4 Further consistency checks

Independent checks can be made into the nature of the star. For example, Kovtyukh et al. (2008) derive a spectroscopic reddening for HD 18391 of  $E(B-V) = 0.991$ , but that is based upon a different adopted  $B-V$  color. With the results of Table 1, the reddening becomes  $E(B-V) = 1.020 \pm 0.003$ . A field reddening for HD 18391 can be found using stars in its immediate vicinity. The observed colors of stars in the 2MASS catalogue (Cutri et al. 2003) lying within  $5'$  of the star are shown in Fig. 7. When analyzed using the method illustrated by Turner et al. (2008), the data imply a field reddening of  $E(J-H) = 0.29 \pm 0.03$ , which corresponds to  $E(B-V) = 1.04 \pm 0.09$ , consistent with the spectroscopic result. The obvious A-type main-sequence stars in the sample have inferred distances of  $\sim 650$  pc, implying that the reddening in the field originates relatively nearby, certainly foreground to the G0 Ia supergiant.

The distance to HD 18391 can be estimated using luminous stars located in close proximity. Table 3 lists early-type and luminous stars located within  $\sim 15'$  of the G0 Ia supergiant from Volume I of *Luminous Stars in the North-*

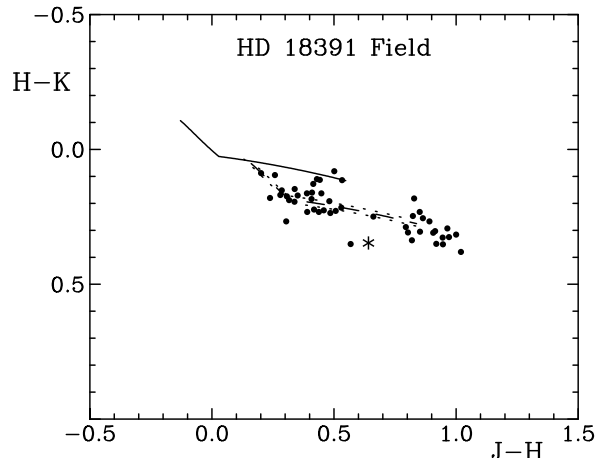


**Fig. 7** A 2MASS color-color diagram,  $H-K$  versus  $J-H$ , for stars within  $5'$  of HD 18391 having magnitude uncertainties less than  $\pm 0.03$ . The intrinsic relation for main-sequence stars is plotted as a solid line, and the same relation reddened by  $E(J-H) = 0.29 \pm 0.03$  as a dashed line surrounded by dotted lines. The kink corresponds to A0 stars. HD 18391 is depicted by an asterisk.

**Table 3** Luminous stars within  $\sim 15'$  of HD 18391.

Star	Sp.T.	$V$	$B-V$	Source	$E(B-V)$	$V_0-M_V$
HD 18391	G0 Ia	6.94	1.97	1	1.02	...
LS+57°111	OB+ce,h	11.42	0.85	2	...	...
LS+57°113	B0.5 V	11.03	0.81	1,2	1.09	11.13
LS+57°114	A2 Ib	11.31	1.00	2	0.95	13.18
LS+57°115	B1.5 Vn	12.46	0.83	1,2	1.08	11.48
3709 490 1	B2 Vnn	11.34	0.60	1,4	0.84	10.83
LS+57°116	b1 v	11.94	0.89	2	1.16	11.21
LS+57°117	B0 V	10.82	0.87	1,2	1.17	10.77
V637 Cas	M2 Iab-Ib	9.88	2.70	3	0.99	11.31
Mean					11.12	
s.e.					$\pm 0.12$	

Sources: 1. This paper, 2. Haug 1970, 3. Lee 1970, 4. Perryman et al. 1997.

ern Milky Way (Hardorp et al. 1959), for which photometric observations are available from Haug (1970), Lee (1970), and Perryman et al. (1997). Included is the LC class variable M supergiant V637 Cas. Spectral types are available for most stars from the ADS database, including results from White & Wing (1978) for V637 Cas, but our spectroscopic observations of the B-type stars, presented in Fig. 8, were used to test and augment them. The resulting spectral classifications produce the spectroscopic distance moduli given in the last column of Table 3, where a value of  $R = A_V/E(B-V) = 3.2$  has been adopted for the ratio of total-to-selective absorption in this region of the Galaxy (Turner 1976).

All of the luminous stars near HD 18391 are reddened by  $E(B-V) \simeq 1.0$ , with distance moduli of  $\sim 11$ . The exception is the A2 Ib supergiant LS+57°114, which does not fit coevally with the remainder of the group. The mean unreddened distance modulus for the group is  $V_0 - M_V =$

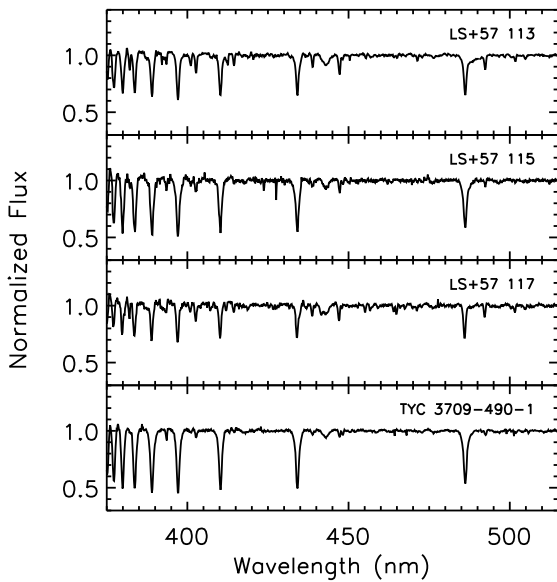


**Fig. 8** Low-dispersion spectra for stars near HD 18391.

$11.12 \pm 0.12$ , corresponding to a distance of  $1678 \pm 96$  pc. Interestingly enough, there is a sparse group of early-type stars located  $\sim 10'$  west of HD 18391 at J2000 co-ordinates 2:58:28, +57:37:30 (Fig. 9). The cluster is only marginally detectable by eye, although similarly sparse groups have been detected previously in such fashion by the lead author (e.g., Turner 1985; Turner et al. 1993). Visually, the cluster displays the characteristics of a loose group in the terminal stages of dissolution into the field, as confirmed by star counts. Ring counts about the adopted cluster center for  $J \leq 15$  are shown in Fig. 10, from which one derives nuclear and coronal radii of  $r_n = 3.5'$  (1.7 pc) and  $R_c = 14'$  (6.8 pc), respectively, in the nomenclature of Kholopov (1969). An unusual feature is the increase in star densities in the cluster corona, indicative of a ringlike feature. A similar characteristic is shared by Collinder 70, better known as the Orion Ring, a young cluster of stars surrounding  $\epsilon$  Ori in Orion's Belt that is in the advanced stages of dissolution into the field.

The parameters for this group of stars, most of which can be identified as early B-type dwarfs from their 2MASS colors (Fig. 11), are similar to those for stars lying closer to HD 18391. The implied reddening is  $E(J - H) = 0.40 \pm 0.02$ , corresponding to  $E(B - V) = 1.43 \pm 0.07$ , and the distance modulus is  $J_0 - M_J = 11.07 \pm 0.15$ , corresponding to a distance of  $1638 \pm 113$  pc. The adopted mean of the two estimates is  $d = 1661 \pm 73$  pc ( $11.10 \pm 0.10$  in intrinsic distance modulus). HD 18391 and most of the luminous stars of Table 3 lie in the cluster corona, a by-now common characteristic of many young star clusters (e.g., Burki 1978a). The predicted number of cluster members for  $J \leq 15$  lying within  $3.5'$  of the cluster center is  $16 \pm 8$  according to the star counts, compared with exactly 16 identified in this region from 2MASS photometry. The total number of

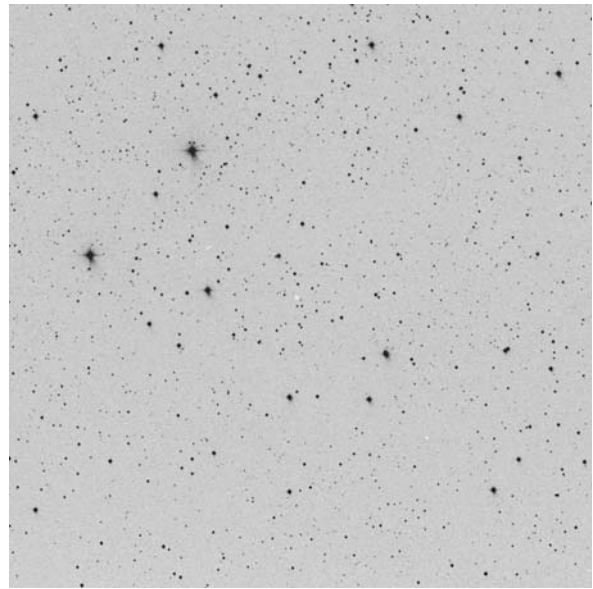


**Fig. 9** The view of the anonymous cluster located at 2:58:28, +57:37:30 (J2000) on the Palomar Observatory Sky Survey blue plate. The field measures  $30' \times 30'$  with north up, and HD 18391 is the bright star on the left edge of the field. [The National Geographic Society–Palomar Observatory Sky Atlas (POSS-1) was made by the California Institute of Technology with grants from the National Geographic Society.]

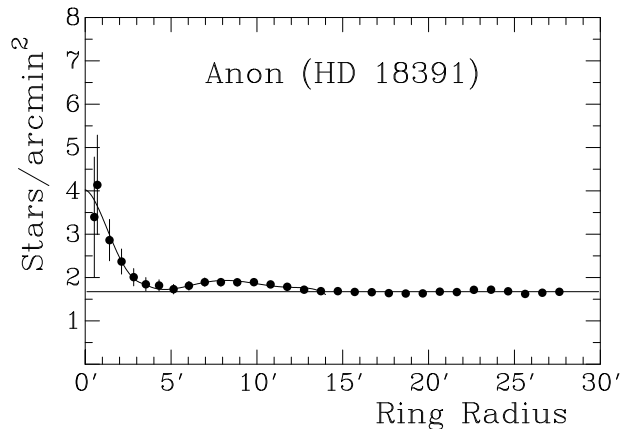


**Fig. 10** Ring counts for  $J \leq 15$ , with their Poisson uncertainties, for the anonymous cluster centered at 2:58:28, +57:37:30 (J2000). The field star level based upon rings with  $r \geq 13'$  is shown, as is a possible trend for cluster stars. The dimensional parameters are  $r_n = 3.5'$  and  $R_c = 14'$ .

cluster members with  $J \leq 15$  according to the star counts is  $102 \pm 35$ , typical of a poorly-populated cluster.

If HD 18391 is a member of the cluster and B-star group, its implied luminosity is  $M_V = -7.76 \pm 0.10$ . It appears to fit in an evolutionary sense as well, according to the unreddened color-magnitude diagram of Fig. 12 for stars in the B-star group. The stars appear to have an age of  $\log t = 6.95 \pm 0.05$ , or  $(9 \pm 1) \times 10^6$  years, according to an isochrone fit to models by Meynet et al. (1993). The irregular M supergiant variable V637 Cas does not match the same

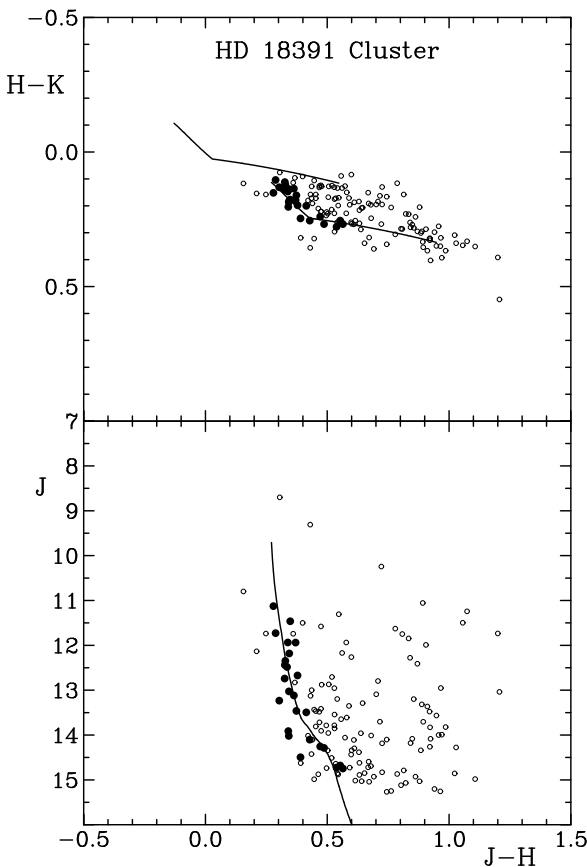


**Fig. 11** A 2MASS color-color diagram,  $H - K$  versus  $J - H$  (upper section), for stars within 5' of 2:58:28, +57:37:30 (J2000) having magnitude uncertainties less than  $\pm 0.05$ . The intrinsic relation for main-sequence stars is plotted as a solid line, as well as for  $E(J - H) = 0.40$ . Filled circles represent likely cluster members, open circles probable field stars. Note the large number of reddened stars blueward of the A0 star kink. The lower section is a color-magnitude diagram for the same stars, indicating the best zero-age main-sequence fit for  $J - M_J = 11.07 \pm 0.15$ .

**Table 4** Radial velocity data.

Star	JD	$V_R$ ( $\text{km s}^{-1}$ )
HD 18391	2449739.3755	-41.3
HD 18391	2452711.3171	-44.4
HD 18391	2453785.2410	-43.5

isochrone very well, almost certainly because of heavy mass loss during its previous evolution (e.g., Jura & Kleinmann 1990). A similar situation applies to the M supergiant BC Cyg as a member of Berkeley 87 (Turner & Forbes 1982; Turner et al. 2006b; Majaess et al. 2008), and the M3 Iab-Ib member of NGC 2439 (Turner 1977). The mass of stars at the red turnoff (RTO) for a  $9 \times 10^6$  year-old cluster is  $18.5 M_\odot$  according to Meynet et al. (1993), implying that the mass of HD 18391 is  $\sim 19 M_\odot$ . Possible membership of HD 18391 in Cas OB6 can be ruled out. Cas OB6 members include evolved O4 and O5 stars (Hillwig et al. 2006), implying a much younger age, and are more distant: 2.01

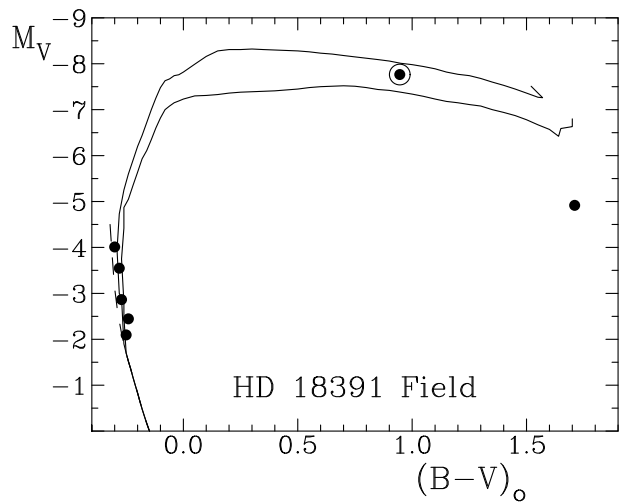


**Fig. 12** An extinction-free H-R diagram for neighboring stars to HD 18391, the circled point. Isochrones are shown for  $\log t = 6.9$  (upper) and  $\log t = 7.0$  (lower).

kpc according to Mel'nik & Efremov (1995),  $\sim 1.9$  kpc as adopted by Hillwig et al. (2006). They also have radial velocities of  $\sim -50 \text{ km s}^{-1}$ , marginally more negative than the measured velocities for HD 18391 summarized in Table 4. Attempts were made to measure radial velocities for the associated B stars observed spectroscopically in Fig. 8, but with negative results because of zero-point problems. The three coolest stars in the sample were found to have nearly identical velocities, however.

The implied luminosity of HD 18391,  $M_V = -7.76$ , or  $M_{\text{bol}} = -7.79$ , agrees closely with expectations from published semi-period-luminosity relations for Cepheid-like supergiants (Burki 1978b), provided that the longer period ( $P = 178$  d) applies. Interestingly enough, both HD 18391 and V810 Cen also fit predictions from the Cepheid period-luminosity relation, as shown in Fig. 13. The results for the two FG class Ia supergiants are based upon their assumed membership in Anon (HD 18391) and Stock 14 (see Turner 1982), although the case for V810 Cen as a cluster member has been questioned on the basis of a conflict with the radial velocity of Stock 14 stars (Keinzel et al. 1998). The case for HD 18391 also requires radial velocity confirmation.

The radius of HD 18391 implied by its luminosity and effective temperature is  $329 R_\odot$ , whereas a value of  $583 R_\odot$  would characterize a Cepheid of the same pulsation period (Turner & Burke 2002). The implied radius also produces a value of  $\log g = 0.69$  with the effective temperature inferred from the model atmosphere analysis (Kovtyukh et al. 2008), consistent with the cited value of  $\log g = 1.2$  when non-LTE and possible mass-loss effects are taken into account. But HD 18391 is clearly not a Cepheid. Its variability presumably originates from pulsation, radial pulsation if the implied periods are correct, highly damped by convection. Variability possibly linked to the rotation of HD 18391 would imply a rotation rate of  $\sim 90 \text{ km s}^{-1}$ , much too large for a star that has expanded by two orders of mag-

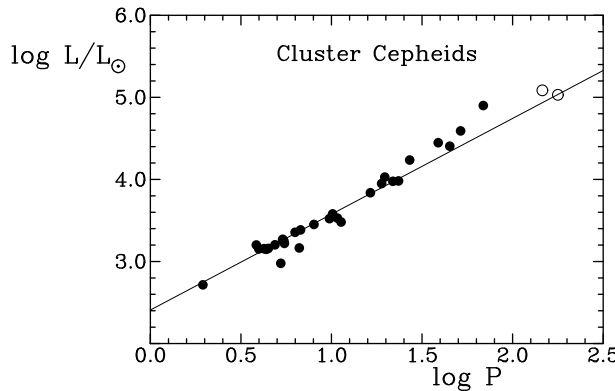


**Fig. 13** The period-luminosity relation for Galactic Cepheids associated with open clusters and associations. Classical Cepheids are denoted by filled circles, and the Cepheid-like supergiants V810 Cen and HD 18391 by open circles.

nitude since the main sequence stage. The color variations of the star are also in antiphase to the brightness variations (Burki 1978b), further constraining the nature of pulsation in the star (Maeder 1980).

## 5 Discussion

The suspected, long-term, low-amplitude, light variability of HD 18391 is confirmed by recent observations of the star, although the light curve derived from recent CCD observations contains considerable scatter, a problem that may be associated with the difficulty of making accurate extinction corrections for observations from a site located near sea level. The dominant period of variability of  $P = 123^{\text{d}}04$  is reasonably solid, but implies a semi-period of  $61^{\text{d}}52$ , smaller than the value of  $\geq 84$  d originally estimated by Rufener et al. (1978). The latter value lies closer to  $P = 177^{\text{d}}84$  (semi-period of  $88^{\text{d}}92$ ) found for the weaker second signal. A luminosity of  $M_V = -7.76$  is implied for HD 18391 from likely membership in a surrounding group of luminous stars that, with the G0 Ia supergiant, are outliers to an anonymous, poorly-populated open cluster  $\sim 10'$  to the west that appears to be dissolving into the field. The likely age of the B-star subgroup surrounding the G0 Ia supergiant is  $\log t = 6.95 \pm 0.05$ , or  $(9 \pm 1) \times 10^6$  years. The luminosity estimate is consistent with the existing semi-period-luminosity relation of Burki (1978b) for such objects.

It is interesting to note that both V810 Cen and HD 18391 fit the period-luminosity relation for cluster and association Cepheids extremely well, in fact unerringly in the case of HD 18391, despite the fact that their implied effective temperatures and luminosities place them well to the hot side of the classical Cepheid instability strip. The mechanism responsible for the variability of such Cepheid impostors is still poorly constrained, although non-radial pulsation and effects tied to mass loss have been considered previously (Maeder 1980). The present results for HD

18391 suggest the possibility of radial pulsation. It is curious how well Cepheid-like supergiants obey the classical period-luminosity relation for Cepheids. It is not clear why that should be, although their presence among the luminous population of galaxies may be important to the identification and use of Cepheids as distance indicators, particularly for low-amplitude variables.

*Acknowledgements.* The authors are grateful to Gilbert Burki for kindly providing unpublished observations of HD 18391 that helped to extend the time baseline of observations for the star.

## References

- Argue, A.N.: 1966, MNRAS 133, 475
- Bessell, M.S.: 2000, PASP 112, 961
- Brown, W.R., Geller, M.J., Kenyon, S.J., Kurtz, M.J.: 2005, ApJ 622, L33
- Burki, G.: 1978a, A&A 62, 159
- Burki, G.: 1978b, A&A 65, 363
- Burki, G.: 2006, JAAVSO 35, 19
- Burki, G.: 2007, private communication
- Burki, G., Maeder, A., Rufener, F.: 1978, A&A 65, 363
- Cutri, R.M., Skrutskie, M.F., van Dyk, S., et al.: 2003, *The IRSA 2MASS All-Sky Point Source Catalog*, NASA/IPAC Infrared Science Archive
- Demarque, P., Virani, S.: 2007, A&A 461, 651
- Fernie, J.D.: 1963, AJ 68, 780
- Fernie, J.D.: 1983, PASP 95, 782
- Foster, G.: 1995, AJ 109, 1889
- Fuentes, C.I., Stanek, K.Z., Gaudi, B.S., McLeod, B.A., Bogdanov, S., Hartman, J.D., Hickox, R.C., Holman, M.J.: 2006, ApJ 636, L37
- Henden, A.A., Munari, U.: 2000, A&AS 143, 343
- Griffin, R.F.: 1970, MNRAS 148, 211
- Haug, U.: 1970, A&AS 1, 35
- Hardorp, J., Rohlfs, K., Slettebak, A., Stock, J.: 1959, *Luminous Stars in the Northern Milky Way I*, Hamburger Sternwarte and Warner and Swasey Observatory
- Hillwig, T.C., Gies, D.R., Bagnulo, Jr., W.G., Huang, W., McSwain, M.V., Wingert, D.W.: 2006, ApJ 639, 1069
- Hoag, A.A., Johnson, H.L., Iriarte, B., Mitchell, R.I., Hallam, K.L., Sharpless, S.: 1961, PUSNO 17, 343
- Imhoff, C.L.: 1977, ApJ 214, 773
- Johnson, H.L.: 1966, ARA&A 4, 193
- Johnson, H.L.: 1968, in: B.M. Middlehurst, L.H. Aller (eds.), *Nebulae and Interstellar Matter*, p. 167
- Jura, M., Kleinmann, S.G.: 1990, ApJS 73, 769
- Keinzel, F., Burki, G., Burnet, M., Meynet, G.: 1998, A&A 337, 779
- Kholopov, P.N.: 1969, SvA 12, 625
- Kovtyukh, V.V.: 2007, MNRAS 378, 617
- Kovtyukh, V.V., Soubiran, C., Bondar, A.V., Korotin, S.A., Musaev, F.A., Yasinskaya, M.P.: 2005, KFNT 21, 141
- Kovtyukh, V.V., Soubiran, C., Luck, R.E., Turner, D.G., Belik, S.I., Andrievsky, S.M., Chekhonadskikh, F.A.: 2008, MNRAS 389, 1336
- Lee, T.A.: 1970, ApJ 162, 217
- Luck, R.E.: 1982, ApJ 263, 215
- Maeder, A.: 1980, A&A 90, 311
- Maeder, A., Rufener, F.: 1972, A&A 20, 437
- Majaess, D.J., Turner, D.G., Lane, D.J., Moncrieff, K.A.: 2008, JAVSO 36, 90

- Mathis, J.S.: 1990, ARA&A 28, 37  
Mel'nik, A.M., Efremov, Yu.N.: 1995, AstL 21, 10  
Meynet, G., Mermilliod, J.-C., Maeder, A.: 1993, A&AS 98, 477  
Nassau, J.J., Morgan, W.W.: 1952, ApJ 115, 475  
Perryman, M.A.C., et al.: 1997, *The Hipparcos and Tycho Catalogues*, ESA SP-1200, ESA, Noordwijk  
Redman, R.O.: 1930, PubDAO 4, 325  
Rufener, F., Bartholdi, P.: 1982, A&AS 48, 503  
Rufener, F., Maeder, A., Burki, G.: 1978, A&AS 31, 179  
Schmidt, E.G.: 1984, ApJS 55, 455  
Stothers, R.: 1972, PASP 84, 373  
Turner, D.G.: 1976, AJ 81, 1125  
Turner, D.G.: 1977, AJ 82, 805  
Turner, D.G.: 1982, PASP 94, 655  
Turner, D.G.: 1985, JRASC 79, 175  
Turner, D.G., Burke, J.F.: 2002, AJ 124, 2931  
Turner, D.G., Forbes, D.: 1982, PASP 94, 789  
Turner, D.G., Abdel-Sabour, Abdel-Latif, M., Berdnikov, L.N.: 2006a, PASP 118, 410  
Turner, D.G., Rohanizadegan, M., Berdnikov, L.N., Pastukhova, E.N.: 2006b, PASP 118, 1533  
Turner, D.G., van den Bergh, S., Younger, P.F., Danks, T.A., Forbes, D.: 1993, ApJS 85, 119  
Turner, D.G., Forbes, D., English, D., et al.: 2008, MNRAS 388, 444  
Vanmunster, T.: 2006, PERANSO Light Curve and Period Analysis Software 2.31, CBA Belgium.com  
Vitense, E.: 1951, ZA 29, 23  
White, N.M., Wing, R.F.: 1978, ApJ 222, 209  
Williams, J.A.: 1966, AJ 71, 615